Inorganic Chemistry

Article

pubs.acs.org/IC

Fluorescent Rhenium-Naphthalimide Conjugates as Cellular Imaging Agents

Emily E. Langdon-Jones,[†] Nadine O. Symonds,[†] Sara E. Yates,[†] Anthony J. Hayes,[‡] David Lloyd,[‡] Rebecca Williams,[‡] Simon J. Coles,[§] Peter N. Horton,[§] and Simon J.A. Pope*[,†]

[†]School of Chemistry, Main Building, Cardiff University, Cardiff CF10 3AT, Cymru/Wales, U.K.

[‡]School of Biosciences, Main Building, Cardiff University, Cardiff CF10 3AT, Cymru/Wales, U.K.

[§]National Crystallographic Service, Chemistry, Faculty of Natural and Environmental Sciences, University of Southampton, Highfield, Southampton, SO17 1BJ, England, U.K.

Supporting Information

ABSTRACT: A range of biologically compatible, fluorescent rhenium-naphthalimide conjugates, based upon the rhenium *fac*-tricarbonyl core, has been synthesized. The fluorescent ligands are based upon a N-functionalized, 4-amino-derived 1,8-naphthalimide core and incorporate a dipicolyl amine binding unit to chelate Re(I); the structural variations accord to the nature of the alkylated imide with ethyl ester glycine ($\mathbf{L^1}$), 3-propanol ($\mathbf{L^2}$), diethylene glycol ($\mathbf{L^3}$), and benzyl alcohol ($\mathbf{L^4}$) variants. The species are fluorescent in the visible region between 505 and 537 nm through a naphthalimide-localized intramolecular charge transfer, with corresponding fluorescent lifetimes of up to 9.8 ns. The ligands and complexes were investigated for their potential as imaging agents for human osteoarthritic cells and protistan fish parasite *Spironucleus vortens* using confocal fluorescence microscopy. The results show that the specific nature of the naphthalimide structure serves to control the uptake and intracellular localization of these imaging agents. Significant differences were noted between the free ligands and complexes, with the Re(I) complex of $\mathbf{L^2}$ showing hydrogenosomal localization in *S. vortens*.

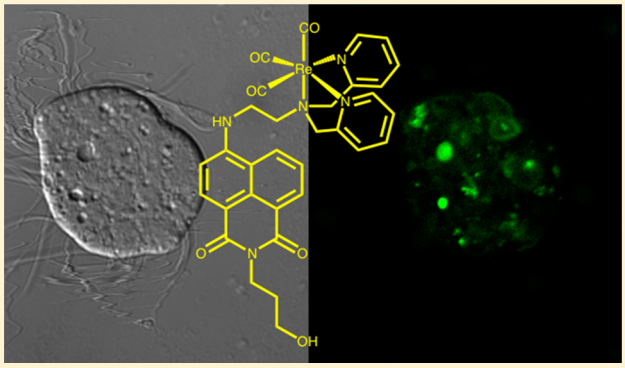

INTRODUCTION

The use of metallo-radionuclides in positron emission tomography (PET) and single photon emission computer tomography (SPECT) is well established, with the metastable isotope ^{99m}Tc ($t_{1/2}$ = 6.01 h, γ = 142.7 keV) a particularly popular choice for the latter. Importantly rhenium also possesses radionuclides $^{186/188}$Re (^{186}Re $t_{1/2}$ = 3.68 d, β = 1.07 MeV, γ = 137 keV; ^{188}Re $t_{1/2}$ = 16.98 h, β = 2.12 MeV, γ = 155 keV), which have promise in radiopharmaceutical therapies.[1] For the application of these radionuclides in synthesis, *fac*-$[M(CO)_3(H_2O)_3]^+$ (M = Tc, Re) is a very convenient precursor for a range of M(I) coordination chemistry and agent production.[2] It is well-known that rhenium is the closest chemical analogue for ^{99m}Tc, and the use of nonradioactive fluorescent Re(I) analogues can obviously help to provide valuable insight with respect to in vivo and in vitro localization characteristics of ^{99m}Tc(I) agents, which are particularly important at the cellular level.[3] The challenge of such an approach is the appropriate design of a biocompatible and kinetically inert complex functionalized with a suitable fluorophore that can be exploited in confocal fluorescence microscopy.

Luminescent organometallic coordination complexes are now well established as viable options for bioimaging applications using confocal fluorescence microscopy.[4] Re(I),[5] Ir(III),[6] and Pt(II)[7] complexes in particular have shown remarkable capability in cellular imaging, with intracellular localization patterns that can be rationalized, and organelle targeting. The added value of a single molecule agent that can simultaneously image and deliver therapeutic activity is significant as such an approach can provide an insight into uptake, distribution, and therapeutic action.[8] For example, coupling anthraquinone fluorophores to Pt(II) complexes has provided models for the investigation of compound distribution in tumors: the anthraquinone fluorophore allows fluorescence microscopy to track the distribution of the complex in cell culture spheroids.[9] Cytotoxic Au(I) complexes have also been functionalized with alkynyl-adorned anthraquinone units and are shown to be very effective cellular imaging agents with modulated antiproliferative activity against a range of cancer cell lines.[10]

Received: January 21, 2014
Published: March 13, 2014

Here we report the use of functionalized naphthalimide-rhenium metal complex fluorophores as excellent agents for cell imaging. The ease with which the substituted 1,8-naphthalimide unit can be functionalized in a stepwise manner should allow exquisite control over the physical properties of the chromophore, including the luminescence characteristics.[11] Critically, the optical properties can be tuned to the visible part of the spectrum by increasing the degree of charge transfer (CT) character in the excited state. Thus, amino-substituted 1,8-naphthalimide fluorophores absorb and emit in the visible region due to N-to-imide CT.[12] The CT character also increases the Stokes shift of the fluorophore, which is advantageous in removing autofluorescence from endogenous fluorophores. The examples of the application of such species to confocal fluorescence microscopy and cellular imaging are rapidly expanding as the broad utility of these fluorophores is realized.[13] A recent comprehensive review by Gunnlaugsson and Kelly has highlighted the breadth of applicability of 1,8-naphthalimide species, including as anticancer agents, DNA binders, and cellular imaging agents.[14] Recent reports have shown that the utility in a biological context is expanding with a number of groups pursuing sensing platforms[15] based upon the 1,8-naphthalimide motif: Zn(II)[16] and Cu(I)[17] imaging agents have been reported using this fluorophore core, albeit relying upon fluorescence intensity change as the prime indicator of sensing.

A small number of naphthalimide-metal complex species have also been reported, often focused upon the development of cancer chemotherapeutic agents. Examples with Pt(II)[18] and Au(I)[19] are known, as well as a number of luminescent Ru(II) species that target DNA binding.[20] Some Ru(II) arene complexes appended with a 1,8-naphthalimide fluorophore also possess very good anticancer activity in drug-resistant cancer cells.[21]

In this Paper we discuss the development of some new dipicolyl amine ligands, which are appended with a N-substituted 1,8-naphthalimide fluorophore, together with their corresponding organometallic Re(I) complexes. These four new complexes are highly fluorescent, kinetically inert, and biologically compatible and have been successfully applied for cellular imaging using confocal fluorescence microscopy.

EXPERIMENTAL SECTION

Diffraction Data Collection and Processing. Diffraction data for $\mathbf{L^1}$ were collected using a standard method[22] on a Rigaku AFC12 goniometer equipped with an enhanced sensitivity (HG) Saturn724+ detector mounted at the window of an FR-E+ SuperBright molybdenum rotating anode generator with HF Varimax optics (100 μm focus) at 100 K. Data collection, data reduction, cell refinement, and absorption correction using CrystalClear-SM Expert 3.1 b26 (Rigaku, 2013). CCDC reference number 981267 contains the supplementary crystallographic data (see Supporting Information) for this Paper.

Structure Analysis and Refinement. The structure was solved by direct methods using SHELXS-97[23] and was completed by iterative cycles of ΔF syntheses and full-matrix least-squares refinement in SHELKX-2013.[23] All non-H atoms were refined anisotropically, and difference Fourier syntheses were employed in positioning idealized hydrogen atoms, which were allowed to ride on their parent C-atoms. The figures was created using the ORTEP3 for Windows.[24]

Human Cell Incubation and Confocal Microscopy. An osteoporetic cell line was maintained in *N*-(2-hydroxyethyl)-piperazine-*N*′-ethanesulfonic acid (Hepes)-modified minimum essential medium (HMEM) supplemented with 10% fetal bovine serum, penicillin, and streptomycin. Cells were detached from the plastic flask using a trypsin−ethylenediaminetetraacetic acid (EDTA) solution and suspended in an excess volume of growth medium. The homogeneous cell suspension was then distributed into 1 mL aliquots, with each aliquot being subject to incubation with a different imaging probe. These luminescent probes were initially dissolved in dimethyl sulfoxide (DMSO) (5 mg/mL) before being added to the cell suspensions, with a final concentration of 100 μg ml^{-1} (corresponding to about 110−190 μM) before incubation at 20 °C for 30 min. Cells were finally washed in phosphate buffer saline (PBS, pH 7.2), removing agent from the medium, then harvested by centrifugation (5 min, 800 g) and mounted on a slide for imaging. Preparations were viewed using a Leica TCS SP2 AOBS confocal laser microscope using ×63 or ×100 objective, with excitation at 405, 488, or 543 nm and detection at 515−600 nm.

General. ^{1}H and ^{13}C{^{1}H} NMR spectra were recorded on an NMR-Fourier transform (FT) Bruker 400 and 250 MHz or Joel Eclipse 300 MHz spectrometer and recorded in $CDCl_3$, CD_3CN, CD_3OD, or $(CD_3)_2CO$. ^{1}H and ^{13}C{^{1}H} NMR chemical shifts (δ) were determined relative to residual solvent peaks with digital locking and are given in ppm. Low-resolution mass spectra were obtained by the staff at Cardiff University. High-resolution mass spectra were carried out at the EPSRC National Mass Spectrometry Service at Swansea University. UV−visible (UV−vis) studies were performed on a Jasco V-570 spectrophotometer as MeCN and MeOH solutions (2.5 or 5 × 10^{-5} M). Photophysical data were obtained on a JobinYvon−Horiba Fluorolog spectrometer fitted with a JY TBX picosecond photodetection module as MeCN solutions. Emission spectra were uncorrected, and excitation spectra were instrument-corrected. The pulsed source was a Nano-LED configured for 295 nm output operating at 1 MHz. Luminescence lifetime profiles were obtained using the JobinYvon−Horiba FluoroHub single photon counting module, and the data fits yielded the lifetime values using the provided DAS6 deconvolution software. Quantum yield measurements were obtained on aerated MeCN solutions of the complexes using $[Ru(bpy)_3](PF_6)_2$ in aerated MeCN as a standard (Φ = 0.016).[25]

All reactions were performed with the use of vacuum line and Schlenk techniques. Reagents were commercial grade and used without further purification. *fac*-$[Re(CO)_3(MeCN)_3]BF_4$[26] and *N*-*tert*-Boc-ethylenediamine[27] were prepared according to the literature.

Synthesis of Compound $\mathbf{Cl^1}$.[28] Triethylamine (1 mL, 7.16 mmol) and 4-chloro-1,8-naphthalic anhydride (1.110 g, 4.77 mmol) were added to a solution of glycine ethyl ester hydrochloride (0.999 g, 7.16 mmol) in ethanol (50 mL). The orange solution was heated at reflux under a dinitrogen atmosphere for 12 h, resulting in the formation of a precipitate. The reaction solution was then cooled, and the solvent was removed in vacuo. The solids were then extracted into dichloromethane and washed with 0.1 M HCl (3 × 20 mL) and water (3 × 20 mL). The organic phase was then dried over $MgSO_4$, filtered, and reduced to a minimal volume. Precipitation with diethyl ether and subsequent filtration and drying afforded $\mathbf{Cl^1}$ as an orange solid. Yield: 0.931 g, 2.93 mmol, 61%. ^{1}H NMR (400 MHz, $CDCl_3$): δ_H = 8.43 (d, 1H, $^3J_{HH}$ = 7.0 Hz, nap), 8.33 (d, 1H, $^3J_{HH}$ = 8.5 Hz, nap), 8.28 (d, 1H, $^3J_{HH}$ = 8.0 Hz, nap), 7.64 (dd, 2H, J_{HH} = 8.0 Hz, 7.5 Hz, nap), 4.81 (s, 2H, NCH_2), 4.17 (q, 2H, $^3J_{HH}$ = 7.0 Hz, OCH_2CH_3), 1.22 (t, 3H, $^3J_{HH}$ = 7.0 Hz, OCH_2CH_3) ppm.

Synthesis of Compound $\mathbf{N^1}$.[29] Compound $\mathbf{Cl^1}$ (0.630 g, 1.98 mmol) and N-*tert*-Boc-ethylenediamine (0.953 g, 5.95 mmol) were heated in dimethylsulfoxide (3 mL) at 70 °C under a nitrogen atmosphere for 12 h. The solution was then allowed to cool and was neutralized with 0.1 M HCl, which induced precipitation of a yellow solid. The crude product was extracted into dichloromethane, washed with water, dried over $MgSO_4$, and filtered. The solvent was reduced to a minimal volume, and precipitation was induced with petroleum ether, allowing subsequent filtration and drying to afford the intermediate product as an orange solid. Yield: 0.521 g, 1.18 mmol, 60%. ^{1}H NMR (400 MHz, $CDCl_3$): δ_H = 8.38 (d, 1H, $^3J_{HH}$ = 8.0 Hz, nap), 8.29 (d, 1H, $^3J_{HH}$ = 8.0 Hz, nap), 8.17 (d, 1H, $^3J_{HH}$ = 8.5 Hz, nap), 7.42 (t, 1H, $^3J_{HH}$ = 8.0 Hz, N*H*), 6.95 (s, 1H, nap), 6.44 (d, 1H, $^3J_{HH}$ = 8.0 Hz, nap), 5.30 (t, 1H, $^3J_{HH}$ = 7.5 Hz, CON*H*), 4.87 (s, 2H, NCH_2), 4.20 (q, 2H, $^3J_{HH}$ = 7.0 Hz, $COCH_2CH_3$), 3.53 (broad app. quin, 2H, $NHCH_2$), 3.36 (broad t, 2H, CH_2CH_2), 1.42 (s, 9H, Bu),

dx.doi.org/10.1021/ic500142z | Inorg. Chem. 2014, 53, 3788−3797

1.25 (t, 3H, $^3J_{HH}$ = 7.0 Hz, OCH_2CH_3) ppm. $^{13}C\{^1H\}$ NMR (75 MHz, $CDCl_3$): δ_C = 169.4 (CO), 164.3 (CO), 163.7 (CO), 157.9, 150.8, 135.0, 131.3, 127.6, 124.6, 122.1, 120.3, 108.7, 103.5, 99.6, 80.4, 61.7, 46.0, 41.3, 39.6, 31.0, 14.3 ppm. Low-resolution mass spectrometry (LRMS) electrospray ionization (ES^-) found: m/z = 440.2 for $[M-H]^-$ and 476.2 for $[M+Cl]^-$.

Trifluoroacetic acid (TFA) (2 mL) was then added dropwise to a solution of the Boc-protected intermediate (0.495 g, 1.12 mmol) in dichloromethane (5 mL) under a nitrogen atmosphere and stirred for 24 h. The solvents were removed under vacuum, with further drying over 30 min. The residue was dissolved in methanol (20 mL) and then dried in vacuo, a process that was repeated in triplicate, to finally afford **N^1** as a hygroscopic yellow solid. ^1H NMR (400 MHz, CD_3OD): δ_H = 8.40 (d, 1H, $^3J_{HH}$ = 8.0 Hz, nap), 8.36 (d, 1H, $^3J_{HH}$ = 7.0 Hz, nap), 8.23 (d, 1H, $^3J_{HH}$ = 8.0 Hz, nap), 7.57 (app. t, 1H, $^3J_{HH}$ = 7.5 Hz, nap), 6.76 (d, 1H, $^3J_{HH}$ = 8.0 Hz, nap), 4.83 (s, 2H, NCH_2), 4.26 (q, 2H, $^3J_{HH}$ = 7.0 Hz, OCH_2CH_3), 3.76 (t, 2H, $^3J_{HH}$ = 5.5 Hz, $NHCH_2$), 3.30−3.37 (m, 4H, $NHCH_2CH_2$), 1.32 (t, 3H, $^3J_{HH}$ = 7.0 Hz, OCH_2CH_3) ppm. $^{13}C\{^1H\}$ NMR (75 MHz, CD_3OD): δ_C = 169.3 (CO), 164.0 (CO), 163.5 (CO) 150.3, 134.2, 130.9, 129.2, 128.0, 124.4, 121.1, 120.3, 108.6, 103.8, 61.4, 40.8, 40.1, 38.2, 13.1 ppm. LRMS (ES^+) found m/z 342.2 for $[M+H]^+$ and 383.2 for $[M+MeCN]^+$.

*Synthesis of Compound **L^1**.* Compound **N^1** (0.176 g, 0.51 mmol) was added to a solution of 2-pyridinecarboxaldehyde (0.1 mL, 1.05 mmol) in 1,2-dichloroethane (15 mL) and stirred for 2 h at room temperature under a nitrogen atmosphere. Sodium triacetoxyborohydride (0.327 g, 1.54 mmol) was then added, and the mixture was stirred for a further 16 h. The solution was then neutralized with saturated aqueous (aq) $NaHCO_3$, and the product was extracted using $CHCl_3$. The organic layer was washed with water (3 × 25 mL) and brine (2 × 25 mL) and then dried over $MgSO_4$. Following filtration, the solvent was removed in vacuo to afford **L^1** as a yellow solid. Yield: 0.133 g, 2.55 mmol, 50%. ^1H NMR (400 MHz, $CDCl_3$): δ_H = 8.79 (d, 1H, $^3J_{HH}$ = 8.5 Hz, nap), 8.56 (d, 1H, $^3J_{HH}$ = 7.0 Hz, nap), 8.51 (d, 2H, $^3J_{HH}$ = 4.5 Hz, py), 8.35 (d, 1H, $^3J_{HH}$ = 8.5 Hz, nap), 7.93 (br t, 1H, N*H*), 7.63 (app. t, 1H, $^3J_{HH}$ = 8.0 Hz), 7.50 (app. t, 2H, $^3J_{HH}$ = 8.0 Hz, py), 7.31 (d, 2H, $^3J_{HH}$ = 8.0 Hz, py), 7.09 (app. t, 2H, $^3J_{HH}$ = 5.5 Hz, py), 6.47 (d, 1H, $^3J_{HH}$ = 8.5 Hz, nap), 4.87 (s, 2H, NCH_2), 4.17 (q, 2H, $^3J_{HH}$ = 7.0 Hz, OCH_2CH_3), 3.95 (s, 4H, NCH_2), 3.38−3.30 (broad m, 2H, $HNCH_2$), 3.00 (t, 2H, $^3J_{HH}$ = 5.0 Hz, $HNCH_2CH_2$), 1.22 (t, 3H, $^3J_{HH}$ = 7.0 Hz, OCH_2CH_3) ppm. $^{13}C\{^1H\}$ NMR (75 MHz, $CDCl_3$): δ_C = 199.3 (CO), 164.7 (CO), 163.8 (CO), 150.9, 149.3, 139.5, 136.8, 135.4, 131.5, 130.5, 128.2, 124.4, 123.5, 122.5, 117.3, 108.0, 104.1, 63.9, 61.4, 60.1, 59.8, 41.3, 41.0, 14.3 ppm. LRMS (ES^+) found m/z 524.5 for $[M+H]^+$, 546.5 for $[M+Na]^+$ and 587.6 for $[M+MeCN+Na]^+$. (High-resolution mass spectroscopy (HRMS) (ES^+) found m/z 524.2285; calculated 524.2292 for $[C_{30}H_{30}O_4N_5]^+$. UV−vis (MeCN): λ_{max} (ε/M^{-1} cm^{-1}) = 439 (13 500), 340 (1100), 324 (1600), 282 (16 000), 269 (15 100), 256 (18 000), 228 (21 500) nm; UV−vis (MeOH): λ_{max} ($\varepsilon/M^{-1}cm^{-1}$) = 445 (13 800), 338 (700), 324 (1600), 282 (18 200), 268 (18 600), 257 (20 700), 228 (16 000), 205 (40 000) nm. IR (solid) ν_{max} = 3302, 2987, 2899, 2848, 1737, 1685, 1641, 1586, 1568, 1549, 1471, 1427, 1400, 1371, 1321, 1302, 1236, 1209, 1136, 1112, 1010, 995, 952, 772, 752 cm^{-1}.

*Synthesis of fac-[Re(CO)$_3$(**L^1**)]BF$_4$ (Re-**L^1**).* Compound **L^1** (57 mg, 0.11 mmol) and *fac*-$[Re(CO)_3(MeCN)_3]BF_4$ (50 mg, 0.10 mmol) were dissolved in $CHCl_3$ (10 mL) and heated at reflux under a nitrogen atmosphere for 18 h. The reaction mixture was allowed to cool, the solvent was reduced to 1−2 mL, and precipitation was induced with the addition of diethyl ether. The product was collected by filtration and washed with diethyl ether, giving the complex as a yellow solid. Yield: 16.7 mg, 19.0 μmol, 18%. ^1H NMR (400 MHz, $(CD_3)_2CO$): δ_H = 8.86 (d, 2H, $^3J_{HH}$ = 8.0 Hz, py), 8.52 (d, 1H, $^3J_{HH}$ = 8.0 Hz, nap), 8.40 (d, 1H, $^3J_{HH}$ = 8.0 Hz, nap), 8.28 (d, 1H, $^3J_{HH}$ = 7.5 Hz, nap), 7.95−7.85 (m, 2H, nap, py), 7.60 (app. t, 1H, $^3J_{HH}$ = 8.5 Hz, nap), 7.56 (d, 2H, $^3J_{HH}$ = 8.0 Hz, py), 7.36 (app. t, 2H, $^3J_{HH}$ = 8.0 Hz, py), 7.19 (br t, 1H, $^3J_{HH}$ = 4.5 Hz, N*H*), 7.02 (d, 1H, $^3J_{HH}$ = 8.0 Hz, nap), 5.36 (d, 2H, $^2J_{HH}$ = 16.5 Hz, 1/2 × $2CH_2$), 5.18 (d, 2H, $^2J_{HH}$ = 16.5 Hz, 1/2 × $2CH_2$), 4.71 (s, 2H, NCH_2CO), 4.40 (t, 2H, $^3J_{HH}$ = 8.0 Hz, NCH_2), 4.20−4.10 (broad m, 2H, NCH_2), 4.07 (q, 2H, $^3J_{HH}$ = 8.5 Hz, OCH_2CH_3), 1.13 (t, 3H, $^3J_{HH}$ = 8.5 Hz, OCH_2CH_3) ppm. LRMS (ES^+) found m/z 794.2 for $[C_{33}H_{29}N_5O_7Re]^+$. HRMS (ES^+) found m/z 792.1587; calculated 792.1591 for $[C_{33}H_{29}N_5O_7Re]^+$. UV−vis (MeCN): λ_{max} (ε/M^{-1} cm^{-1}) 421 (12 800), 338 (2300), 321 (4100), 277 (26 300), 255 (23 700), 228 (24 600) nm. UV−vis (MeOH): λ_{max} (ε/M^{-1} cm^{-1}) 427 (13 100), 339 (2500), 322 (4400), 277 (25 900), 255 (24 200), 228 (24 100), 203 (55 900) nm. IR (solid) ν(CO) = 2031, 1930, 1903, 1676, 1639, 1587 cm^{-1}.

*Synthesis of Compound **Cl^2**.* Prepared as for compound **Cl^1** but using 3-aminopropanol (0.48 mL, 6.13 mmol) and 4-chloro-1,8-naphthalic anhydride (0.713 g, 3.06 mmol) to give **Cl^2** as an orange solid. Yield: 0.662 g, 2.29 mmol, 75%. ^1H NMR (250 MHz, $CDCl_3$): δ_H = 8.61 (d, 1H, $^3J_{HH}$ = 7.5 Hz, nap), 8.56 (d, 1H, $^3J_{HH}$ = 8.5 Hz, nap), 8.45 (d, 1H, $^3J_{HH}$ = 8.0 Hz, nap), 7.83−7.76 (m, 2H, nap), 4.27 (t, 2H, $^3J_{HH}$ = 6.0 Hz, CH_2OH), 3.53 (broad t, 2H, NCH_2CH_2), 3.04 (broad s, 1H, O*H*), 1.92 (app. quin, 2H, $^3J_{HH}$ = 6.0 Hz, NCH_2CH_2) ppm.

*Synthesis of Compound **N^2**.* Prepared as for compound **N^1** but using **Cl^2** (0.510 g, 1.76 mmol) and *N-tert*-Boc-ethylenediamine (0.841 g, 5.25 mmol), giving the intermediate as an orange oil. Yield: 0.649 g, 1.57 mmol, 89%. ^1H NMR (400 MHz, $CDCl_3$): δ_H = 8.35 (d, 1H, $^3J_{HH}$ = 7.0 Hz, nap), 8.18 (d, 1H, $^3J_{HH}$ = 8.5 Hz, nap), 8.14 (d, 1H, $^3J_{HH}$ = 8.5 Hz), 7.43 (app. t, 1H, $^3J_{HH}$ = 7.5 Hz, nap), 7.15 (broad s, 1H, N*H*), 6.38 (d, 1H, $^3J_{HH}$ = 8.5 Hz, nap), 5.97 (broad s, 1H, NHCO), 4.21 (t, 2H, $^3J_{HH}$ = 6.0 Hz, CH_2OH), 3.93 (broad s, 1H, O*H*), 3.58−3.52 (broad m, 2H, naph-$NHCH_2$), 3.52 (t, 2H, $^3J_{HH}$ = 5.5 Hz, NCH_2), 3.37 (app. broad s, 2H, CH_2NHCO), 1.91 (app. quin, 2H, $^3J_{HH}$ = 6.0 Hz, CH_2CH_2OH), 1.42 (s, 9H, Bu) ppm.

Deprotection of the intermediate with TFA in dichloromethane yielded **N^2** as a hygroscopic yellow solid. ^1H NMR (400 MHz, CD_3OD): δ_H = 8.52 (app. t, 2H, $^3J_{HH}$ = 8.0 Hz, nap), 8.38 (d, 1H, $^3J_{HH}$ = 8.5 Hz, nap), 7.69 (app t, 1H, $^3J_{HH}$ = 7.5 Hz, nap), 6.89 (d, 1H, $^3J_{HH}$ = 8.5 Hz, nap), 4.48 (t, 2H, $^3J_{HH}$ = 6.0 Hz, $NHCH_2$), 4.28 (t, 2H, $^3J_{HH}$ = 7.0 Hz, CH_2OH), 3.81 (t, 2H, $^3J_{HH}$ = 6.5 Hz, NCH_2), 3.36 (t, 2H, $^3J_{HH}$ = 6.5 Hz, CH_2NH_2), 2.20 (app. quin, 2H, $^3J_{HH}$ = 6.5 Hz, CH_2CH_2OH) ppm.

*Synthesis of Compound **L^2**.* Prepared as for compound **L^1** but using 2-pyridinecarboxaldehyde (0.39 mL, 4.05 mmol), compound **N^2** (0.605 g, 1.94 mmol), and sodium triacetoxyborohydride (1.23 g, 5.82 mmol), yielding a crude product. The product was extracted into 0.1 M HCl, washed with dichloromethane (20 mL), neutralized, and then re-extracted into dichloromethane, which was removed under vacuum to give **L^2** as an orange oil. Yield: 366 mg, 0.74 mmol, 38%. ^1H NMR (400 MHz, $CDCl_3$): δ_H = 8.73 (d, 1H, $^3J_{HH}$ = 8.5 Hz), 8.48−8.44 (m, 3H, nap, py), 8.23 (d, 1H, $^3J_{HH}$ = 8.5 Hz, nap), 7.92 (s, 1H, N*H*), 7.57 (app. t, 1H, $^3J_{HH}$ = 7.5 Hz, nap), 7.45 (app. t, 2H, $^3J_{HH}$ = 7.5 Hz, py), 7.26 (d, 2H, $^3J_{HH}$ = 8.0 Hz, py), 7.03 (app. t, 2H, $^3J_{HH}$ = 5.5 Hz, py), 6.37 (d, 1H, $^3J_{HH}$ = 8.5 Hz, nap), 4.20 (t, 2H, $^3J_{HH}$ = 5.5 Hz, CH_2OH), 3.88 (s, 4H, CH_2), 3.47 (t, 2H, $^3J_{HH}$ = 5.5 Hz), 3.30−3.25 (broad m, 2H, CH_2), 2.92 (t, 2H, $^3J_{HH}$ = 5.0 Hz, CH_2), 1.86 (app. quin, 2H, $^3J_{HH}$ = 5.5 Hz, CH_2CH_2OH) ppm. $^{13}C\{^1H\}$ NMR (75 MHz, $CDCl_3$): δ_C = 165.3 (CO), 164.7 (CO), 159.5, 158.7, 150.8, 149.1, 149.0, 136.7, 135.1, 131.3, 128.1, 124.3, 123.4, 122.4, 122.3, 120.7, 108.3, 104.0, 59.6, 58.9, 51.0, 41.0, 36.5, 31.1 ppm. LRMS (ES^+) found m/z 495.2 for $[M]^+$. HRMS (ES^+) found m/z = 496.2335 for $[C_{29}H_{29}N_5O_3 + H]^+$, calculated 496.2343 for $[C_{29}H_{29}N_5O_3 + H]^+$. UV−vis (MeCN): λ_{max} (ε/M^{-1} cm^{-1}) 437 (13 100), 339 (700), 324 (1300), 281 (17 200), 260 (22 500), 228 (18 200) nm. UV−vis (MeOH): λ_{max} (ε/M^{-1} cm^{-1}) = 431 (12 900), 339 (1000), 323 (1400), 277 (13 100), 257 (21 600), 226 (16 000), 203 (46 800) nm. IR (solid) ν_{max} = 3267 (br), 2852, 1680, 1641, 1584, 1549, 1476, 1429, 1395, 1331, 1259, 1242, 1140, 1115, 1049, 995, 922, 772, 750 cm^{-1}.

*Synthesis of fac-[Re(CO)$_3$(**L^2**)]BF$_4$ (Re-**L^2**).* Prepared as for *fac*-$[Re(CO)_3(\mathbf{L^1})]BF_4$ but using compound **L^2** (53.6 mg, 0.11 mmol) and *fac*-$[Re(CO)_3(MeCN)_3]BF_4$ (48.0 mg, 0.10 mmol) to give Re-**L^2** as a yellow solid. Yield: 61.9 mg, 72.6 μmol, 73%. ^1H NMR (400 MHz, CD_3CN): δ_H = 8.82 (d, 2H, $^3J_{HH}$ = 5.5 Hz, py), 8.53 (d, 1H, $^3J_{HH}$ = 7.5 Hz, nap), 8.42 (app. d, 2H, $^3J_{HH}$ = 8.5 Hz, nap), 7.92 (app. t, 2H, $^3J_{HH}$ = 8.0 Hz, py), 7.73 (app. t, 1H, $^3J_{HH}$ = 7.5 Hz, nap), 7.49 (d, 2H, $^3J_{HH}$

dx.doi.org/10.1021/ic500142z | Inorg. Chem. 2014, 53, 3788−3797

= 8.0 Hz, py), 7.34 (app. t, 2H, $^3J_{HH}$ = 6.5 Hz, py), 6.95 (d, 1H, $^3J_{HH}$ = 8.5 Hz, nap), 6.37 (br t, 1H, N*H*), 4.99 (d, 2H, $^2J_{HH}$ = 16.5 Hz, 1/2 × 2CH_2), 4.90 (d, 2H, $^2J_{HH}$ = 16.5 Hz, 1/2 × 2CH_2), 4.25 (t, 2H, $^3J_{HH}$ = 7.5 Hz, CH_2), 4.19 (t, 2H, $^3J_{HH}$ = 5.5 Hz, CH_2), 4.01 (app. q, 2H, CH_2), 3.55 (t, 2H, $^3J_{HH}$ = 6.0 Hz), 1.87 (app. quin, 2H, $^3J_{HH}$ = 6.0 Hz, CH_2CH_2OH) ppm. LRMS (ES$^+$) found *m*/*z* 766.1 for [M]$^+$. HRMS (ES$^+$) found *m*/*z* 764.1639; calculated 764.1642 for [$C_{32}H_{29}N_5O_6Re$]$^+$. UV−vis (MeCN): λ_{max} (ε/M^{-1} cm^{-1}) = 421 (13 800), 338 (4400), 323 (6100), 272 (35 600), 258 (35 600); UV−vis (MeOH): λ_{max} (ε/M^{-1} cm^{-1}) 427 (13 000), 337 (3300), 324 (4800), 272 (29 700), 258 (30 900), 227 (26 200), 203 (59 200) nm. IR (solid) ν(CO) = 2025, 1921, 1898, 1690, 1629 cm^{-1}.

Synthesis of Compound ***Cl**³*. Prepared as for compound **Cl**¹, using 2-(2-aminoethyl)ethanol (0.80 mL, 8.04 mmol) and 4-chloro-1,8-naphthalic anhydride (0.935 g, 4.02 mmol) to give **Cl**³ as an orange solid. Yield: 1.065 g, 3.33 mmol, 83%. ^{1}H NMR (250 MHz, $CDCl_3$): δ_H = 8.53 (d, 1H, $^3J_{HH}$ = 8.5 Hz, nap), 8.45 (d, 1H, $^3J_{HH}$ = 9.5 Hz, nap), 8.37 (d, 1H, $^3J_{HH}$ = 8.0 Hz, nap), 7.72 (app. t, 1H, $^3J_{HH}$ = 7.5 Hz, nap), 7.69 (d, 1H, $^3J_{HH}$ = 8.0 Hz, nap), 4.34 (t, 2H, $^3J_{HH}$ = 5.5 Hz, NCH_2), 3.77 (t, 2H, $^3J_{HH}$ = 5.5 Hz, CH_2OH), 3.62−3.55 (m, 4H, CH_2OCH_2), 2.56 (s, 1H, O*H*) ppm.

Synthesis of Compound ***N**³*. Prepared as for compound **N**¹, but using **Cl**³ (0.401 g, 1.25 mmol) and *N*-*tert*-Boc-ethylenediamine (0.601 g, 3.75 mmol), affording the intermediate as a solid. Yield: 0.492 g, 1.11 mmol, 89%. ^{1}H NMR (400 MHz, $CDCl_3$): δ_H = 8.00 (d, 1H, $^3J_{HH}$ = 8.0 Hz, nap), 7.90 (d, 1H, $^3J_{HH}$ = 7.0 Hz, nap), 7.84 (d, 1H, $^3J_{HH}$ = 8.0 Hz), 7.12 (app. t, 1H, $^3J_{HH}$ = 7.0 Hz, N*H*), 6.79 (s, 1H, nap), 6.24 (app. s, 1H, N*H*CO), 6.11 (d, 1H, $^3J_{HH}$ = 8.0 Hz, nap), 4.20 (app. br s, 2H, CH_2), 3.73 (br t, 2H, CH_2), 3.66 (app. br s, 2H, CH_2), 3.59 (app. br s, 2H, CH_2), 3.42 (app. br s, 2H, CH_2), 3.19 (app. br s, 2H, CH_2), 1.36 (s, 9H, Bu) ppm.

Deprotection of the intermediate with TFA, followed by work up yielded **N**³ as a hygroscopic orange solid. ^{1}H NMR (400 MHz, CD_3OD): δ_H = 8.51 (d, 1H, $^3J_{HH}$ = 8.0 Hz, nap), 8.45 (d, 1H, $^3J_{HH}$ = 8.0 Hz, nap), 8.26 (d, 1H, $^3J_{HH}$ = 8.5 Hz, nap), 7.59 (app. t, 1H, $^3J_{HH}$ = 8.0 Hz, nap), 6.80 (d, 1H, $^3J_{HH}$ = 8.5 Hz, nap), 4.47 (app. t, 2H, $^3J_{HH}$ = 4.5 Hz, CH_2), 4.32−4.28 (m, 4H, CH_2), 3.84−3.77 (m, 4H, CH_2), 3.36 (t, 2H, $^3J_{HH}$ = 7.5 Hz, CH_2) ppm. ^{13}C{^{1}H} NMR (75 MHz, CD_3OD): δ_C = 164.7 (CO), 164.2 (CO), 150.2 (CO), 134.2, 130.9, 127.9, 124.5, 122.0, 120.6, 109.4, 108.0, 104.1, 103.9, 84.1, 72.1, 67.9, 60.9, 39.8, 38.2, 37.6 ppm. LRMS (ES$^+$) found *m*/*z* 344.3 for [M+H]$^+$, 366.3 for [M+Na]$^+$ and 407.3 for [M+MeCN+Na]$^+$.

Synthesis of Compound ***L**³*. Prepared as for compound **L**¹, but using 2-pyridinecarboxaldehyde (70 μL, 0.76 mmol), compound **N**³ (0.128 g, 0.37 mmol), and sodium triacetoxyborohydride (0.237 g, 1.12 mmol) to give **L**³ as an orange solid. Yield: 35.6 mg, 67.5 μmol, 18%. ^{1}H NMR (400 MHz, $CDCl_3$): δ_H = 8.77 (d, 1H, $^3J_{HH}$ = 8.5 Hz, nap), 8.56 (d, 1H, $^3J_{HH}$ = 6.5 Hz, nap), 8.51 (d, 2H, $^3J_{HH}$ = 4.0 Hz, py), 8.34 (d, 1H, $^3J_{HH}$ = 8.5 Hz, nap), 7.88 (s, 1H, N*H*), 7.62 (app. t, 1H, $^3J_{HH}$ = 8.0 Hz, nap), 7.50 (app. t, 2H, $^3J_{HH}$ = 8.5 Hz, py), 7.31 (d, 2H, $^3J_{HH}$ = 8.0 Hz, py), 7.09 (app. t, 2H, $^3J_{HH}$ = 6.0 Hz, py), 6.47 (d, 1H, $^3J_{HH}$ = 8.5 Hz, nap), 4.37 (t, 2H, $^3J_{HH}$ = 5.5 Hz, NCH_2), 3.95 (s, 4H, NCH_2), 3.79 (t, 2H, $^3J_{HH}$ = 5.5 Hz), 3.65−3.61 (m, 4H, CH_2), 3.40−3.30 (broad m, 2H, CH_2), 2.99 (t, 2H, $^3J_{HH}$ = 5.5 Hz, CH_2) ppm. ^{13}C{^{1}H} NMR (75 MHz, $CDCl_3$): δ_C = 187.6, 167.6 (CO), 164.2 (CO), 158.8, 151.5, 149.3, 143.9, 139.8, 137.3, 136.8, 135.7, 128.1, 123.4, 122.5, 107.5, 104.1, 81.3, 59.8, 23.0, 21.9, 20.5, 17.4, 13.8, 5.9 ppm. LRMS (ES$^+$) found *m*/*z* 526.2 for [M+H]$^+$ and 548.2 for [M+Na]$^+$. HRMS (ES$^+$) found *m*/*z* 560.2053; calculated 560.2047 for [$C_{30}H_{31}O_4N_5$ + Cl]. UV−vis (MeCN): λ_{max} (ε/M^{-1} cm^{-1}) 437 (14 400), 340 (1000), 324 (1500), 280 (20 800), 260 (24 400), 228 (18 700) nm. IR (solid) ν_{max} = 3208 (br), 2893, 2864, 1684, 1641, 1589, 1556, 1476, 1429, 1368, 1327, 1304, 1234, 1117, 1051, 1003, 885, 772, 756 cm^{-1}.

*Synthesis of fac-[Re(CO)₃(**L**³)]BF₄ (Re-**L**³).* Prepared as for *fac*-[Re(CO)$_3$(L^1)]BF$_4$, but using compound **L**³ (16.8 mg, 32.0 μmol) and *fac*-[Re(CO)$_3$(MeCN)$_3$]BF$_4$ (14.6 mg, 30.4 μmol) to give a yellow solid. Yield: 15.5 mg, 17.6 μmol, 58%. ^{1}H NMR (400 MHz, $CDCl_3$): δ_H = 8.59 (d, 2H, $^3J_{HH}$ = 5.5 Hz, py), 8.36−8.30 (m, 3H, nap, py), 7.79−7.69 (m, 2H, nap), 7.66 (d, 2H, $^3J_{HH}$ = 8.0 Hz, py), 7.49 (app. t, 1H, $^3J_{HH}$ = 8.0 Hz, nap), 7.14 (app. t, 2H, $^3J_{HH}$ = 6.0 Hz, py), 6.78 (br t, 1H, $^3J_{HH}$ = 8.5 Hz, N*H*), 6.67 (d, 1H, $^3J_{HH}$ = 8.0 Hz, nap), 5.53 (d, 2H, $^2J_{HH}$ = 16.5 Hz, 1/2 × 2CH_2), 4.58 (d, 2H, $^2J_{HH}$ = 16.5 Hz, 1/2 × 2CH_2), 4.34 (t, 2H, $^3J_{HH}$ = 5.0 Hz, NCH_2), 4.18 (t, 2H, $^3J_{HH}$ = 5.0 Hz, CH_2), 4.10−4.02 (m, 2H, CH_2), 3.83 (t, 2H, $^3J_{HH}$ = 5.5 Hz, NCH_2), 3.70−3.48 (m, 4H, OCH_2). LRMS (ES$^+$) found *m*/*z* 796.4 for [M]$^+$. HRMS (ES$^+$) found *m*/*z* 794.1741; calculated 794.1748 for [$C_{33}H_{31}N_5O_7Re$]$^+$. UV−vis (MeCN): λ_{max} (ε/M^{-1} cm^{-1}) = 421 (12 800), 338 (2300), 321 (4100), 277 (26 300), 255 (23 700), 228 (24 600) nm. UV−vis (MeOH): λ_{max} (ε/M^{-1} cm^{-1}) = 427 (15 200), 338 (5000), 323 (6600), 277 (28 000), 258 (29 600), 227 (28 000), 203 (62 300) nm. IR (solid) ν(CO) = 2031, 1910 (br), 1690, 1643 cm^{-1}.

Synthesis of Compound ***Cl**⁴*. Prepared as for compound **Cl**¹, but using 4-chloro-1,8-naphthalic anhydride (0.144 g, 0.62 mmol), 3-aminobenzyl alcohol (0.304 g, 2.47 mmol), and triethylamine (0.14 mL, 0.926 mmol) to afford **Cl**⁴ as a yellow solid. Yield: 132 mg, 0.39 mmol, 63%. ^{1}H NMR (250 MHz, $CDCl_3$): δ_H = 8.69 (d, 1H, $^3J_{HH}$ = 7.5 Hz, nap), 8.60 (d, 1H, $^3J_{HH}$ = 7.5 Hz, nap), 8.44 (d, 1H, $^3J_{HH}$ = 8.0 Hz, nap), 7.90−7.76 (m, 2H, Ph), 7.51−7.35 (m, 2H, nap, Ph), 7.26 (s, 1H, Ph), 7.20−7.08 (d, 1H, nap), 4.68 (s, 2H, CH_2OH) ppm.

Synthesis of Compound ***N**⁴*. Prepared as for compound **N**¹, but using **Cl**⁴ (0.619 g, 1.83 mmol) and N-*tert*-Boc-ethylenediamine (0.881 g, 5.50 mmol). The intermediate was isolated as a sticky orange solid. Yield: 0.810 g, 1.76 mmol, 96%. ^{1}H NMR (250 MHz, $CDCl_3$): δ_H = 8.59 (d, 1H, $^3J_{HH}$ = 7.0 Hz, nap), 8.46 (d, 1H, $^3J_{HH}$ = 8.5 Hz, nap), 8.33 (d, 1H, $^3J_{HH}$ = 8.5 Hz, nap), 7.61 (app. t, 1H, $^3J_{HH}$ = 8.0 Hz, nap), 7.52−7.40 (m, 2H, Ph), 7.35 (s, 1H, Ph), 7.28 (d, 1H, $^3J_{HH}$ = 8.0 Hz, Ph), 7.22 (br t, 1H, N*H*), 6.59 (d, 1H, $^3J_{HH}$ = 8.5 Hz, nap), 5.23 (t, 1H, $^3J_{HH}$ = 6.5 Hz, N*H*CO), 4.77 (s, 2H, CH_2OH), 3.73−3.63 (br m, 2H, NHCH_2), 3.50−3.46 (br m, 2H, CH_2NHCO), 2.27 (br s, 1H, O*H*), 1.51 (s, 9H, Bu) ppm.

Deprotection of the intermediate with TFA, followed by work up yielded **N**² as a hygroscopic yellow oil. ^{1}H NMR (400 MHz, CD_3OD): δ_H = 8.27 (d, 1H, $^3J_{HH}$ = 8.5 Hz, nap), 8.18 (d, 1H, $^3J_{HH}$ = 8.0 Hz, nap), 8.09 (d, 1H, $^3J_{HH}$ = 8.5 Hz, nap), 7.48−7.23 (m, 3H, nap, Ph), 7.17 (s, 1H, Ph), 7.05 (d, 1H, $^3J_{HH}$ = 7.0 Hz, Ph), 6.60 (d, 1H, $^3J_{HH}$ = 9.0 Hz, nap), 4.55 (s, 2H, CH_2OH), 3.62 (t, 2H, $^3J_{HH}$ = 6.0 Hz, CH_2CH_2), 3.19 (br s, 2H) ppm.

Synthesis of Compound ***L**⁴*. Prepared as for compound **L**¹ but using 2-pyridinecarboxaldehyde (0.32 mL, 3.35 mmol), compound **N**⁴ (0.590 g, 1.63 mmol), and sodium triacetoxyborohydride (1.13 g, 4.85 mmol) to give crude **L**⁴ as an orange oil. The product was purified via column chromatography, first eluting with dichloromethane and then collecting the product by eluting with 3% MeOH in dichloromethane. Yield: 149 mg, 0.74 mmol, 17%. ^{1}H NMR (400 MHz, $CDCl_3$): δ_H = 8.77 (d, 1H, $^3J_{HH}$ = 8.5 Hz, nap), 8.53 (d, 1H, $^3J_{HH}$ = 7.0 Hz, nap), 8.46 (d, 2H, $^3J_{HH}$ = 4.5 Hz, py), 8.30 (d, 1H, $^3J_{HH}$ = 8.5 Hz, nap), 7.89 (br s, 1H, N*H*), 7.61 (app. t, 1H, $^3J_{HH}$ = 8.0 Hz, nap), 7.50−7.31 (m, 4H, nap, Ph, py), 7.29 (d, 2H, $^3J_{HH}$ = 8.0 Hz, py), 7.25 (s, 1H, Ph), 7.15 (d, 1H, $^3J_{HH}$ = 7.5 Hz, nap), 7.05 (app. t, 2H, $^3J_{HH}$ = 6.5 Hz, py), 6.44 (d, 1H, $^3J_{HH}$ = 8.5 Hz, nap), 4.66 (s, 2H, HOCH_2), 3.89 (s, 4H, NCH_2), 3.40−3.25 (broad m, 2H, CH_2), 2.93 (t, 2H, $^3J_{HH}$ = 5.0 Hz, CH_2), 2.61 (broad s, 1H, O*H*) ppm. ^{13}C{^{1}H} NMR (75 MHz, $CDCl_3$): δ_C = 165.2, 164.4, 158.8, 150.9, 149.2, 142.8, 136.8, 135.3, 131.5, 129.4, 128.3, 127.9, 127.4, 126.9, 124.4, 123.5, 122.9, 122.5, 121.0, 108.7, 104.1, 64.7, 59.8, 51.2, 41.0 ppm. LRMS (ES$^+$) found *m*/*z* 526.2 for [M+H]$^+$ and 548.2 for [M+Na]$^+$. HRMS (ES$^+$) found *m*/*z* = 544.2338; calculated 544.2343 for [$C_{33}H_{29}N_5O_3$ + H]$^+$. UV−vis (MeCN): λ_{max} (ε/M^{-1} cm^{-1}) 436 (14 900), 341 (1000), 325 (1700), 282 (18 100), 265 (19 500), 226 (22 200) nm. UV−vis (MeOH): λ_{max} (ε/M^{-1} cm^{-1}) 445 (14 200), 339 (900), 323 (2000), 282 (16 200), 268 (17 800), 261 (18 000), 227 (20 300), 203 (61 500) nm. IR (solid) ν_{max} = 3260 (br), 2830, 1688, 1641, 1576, 1539, 1433, 1358, 1260, 1240, 1146, 1003, 766, 754 cm^{-1}.

*Synthesis of fac-[Re(CO)₃(**L**⁴)]BF₄ (Re-**L**⁴).* Prepared as for [Re(CO)$_3$(**L**^{1})]BF$_4$, but using compound **L**⁴ (30.2 mg, 55.6 μmol) and [Re(CO)$_3$(MeCN)$_3$]BF$_4$ (25.9 mg, 54.0 μmol) to give a yellow solid. Yield: 33.4 mg, 37.1 μmol, 69%. ^{1}H NMR (400 MHz, CD_3CN): δ_H = 8.82 (d, 2H, $^3J_{HH}$ = 5.5 Hz, py), 8.56 (d, 1H, $^3J_{HH}$ = 8.0 Hz, nap), 8.49 (d, 1H, $^3J_{HH}$ = 8.5 Hz, nap), 8.45 (d, 1H, $^3J_{HH}$ = 8.0 Hz, nap), 7.92

dx.doi.org/10.1021/ic500142z | *Inorg. Chem.* 2014, 53, 3788−3797

(app. t, 2H, $^3J_{HH}$ = 8.0 Hz, py), 7.78 (app. t, 1H, $^3J_{HH}$ = 7.5 Hz, nap), 7.55−7.40 (m, 4H, nap, Ph), 7.38−7.32 (m, 3H, py, Ph), 7.23 (d, 1H, $^3J_{HH}$ = 8.0 Hz, Ph), 7.01 (d, 1H, $^3J_{HH}$ = 8.5 Hz, nap), 6.42 (t, 1H, $^3J_{HH}$ = 8.0 Hz, N*H*), 4.98 (d, 2H, $^2J_{HH}$ = 17.0 Hz, 1/2 × 2CH_2), 4.90 (d, 2H, $^2J_{HH}$ = 17.0 Hz, 1/2 × 2CH_2), 4.68 (s, 2H), 4.26 (t, 2H, $^3J_{HH}$ = 6.0 Hz, CH_2), 4.10−4.02 (m, 2H, CH_2) ppm. LRMS (ES$^+$) found: m/z 766.1 for [M]$^+$. HRMS (ES$^+$) found m/z 812.1642; calculated 812.1642 for $[C_{36}H_{29}O_6N_5Re]^+$. UV−vis (MeCN): λ_{max} (ε/M^{-1} cm^{-1}) 420 (15 200), 338 (3200), 321 (4800), 312 (4600), 276 (11 100), 256 (13 400), 226 (33 500) nm. UV−vis (MeOH): λ_{max} (ε/M^{-1} cm^{-1}) 427 (17 900), 336 (4100), 322 (6100), 270 (32 600), 205 (81 400) nm. IR (solid) ν(CO) = 2029, 1906, 1682, 1640 cm^{-1}.

RESULTS AND DISCUSSION

Synthesis and Characterization. The ligands ($\mathbf{L}^{1-4}$) were isolated in four steps (Scheme 1) from commercially available

Scheme 1. Synthetic Route to the Ligands and Complexes[a]

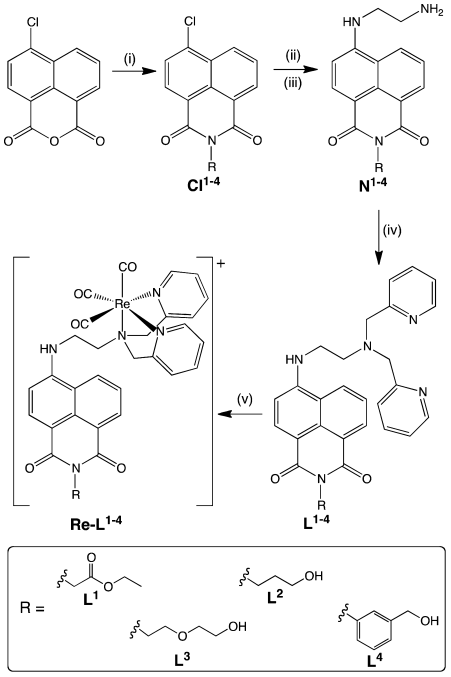

[a](i) RNH$_2$, EtOH; (ii) Boc-NH(CH$_2$)$_2$NH$_2$, DMSO; (iii) TFA, dichloromethane; (iv) 2-pyridinecarboxaldehyde, NaBH(OAc)$_3$, 1,2-dichloroethane; (v) *fac*-[Re(CO)$_3$(MeCN)$_3$](BF$_4$), CHCl$_3$.

4-chloro-1,8-naphthalic anhydride. First, conversion to the chloro-substituted naphthalimide species ($\mathbf{Cl}^{1-4}$) was easily achieved by heating the appropriate amine in ethanol. Subsequent reaction of this intermediate with *N-tert*-Boc-ethylenediamine in DMSO, followed by TFA-mediated deprotection, yielded the amino-derived pro-ligand, $\mathbf{N}^{1-4}$. A one-pot reductive amination procedure using 2-pyridinecarboxaldehyde gave the desired dipicolylamine binding site.[30] The four ligands, incorporating glycine ethyl ester ($\mathbf{L}^1$), propyl alcohol ($\mathbf{L}^2$), ethylene glycol ($\mathbf{L}^3$), and benzyl alcohol ($\mathbf{L}^4$), were fully characterized via NMR spectroscopy and MS studies.

In addition to the solution-state characterization, a single-crystal structural determination (Figure 1) was obtained for $\mathbf{L}^1$. The data collection parameters (Table S1) are presented in the Supporting Information. The data shows the anticipated structure.

The four ligands were each reacted with *fac*-[Re(CO)$_3$(MeCN)$_3$](BF$_4$) in refluxing chloroform to yield the

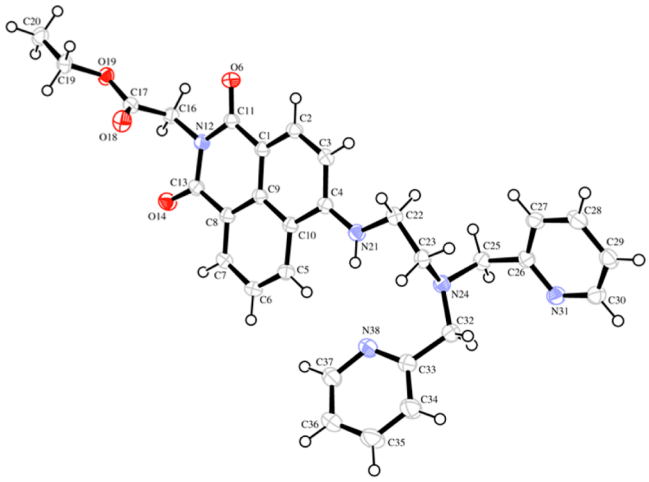

Figure 1. X-ray crystal structure of $\mathbf{L}^1$ with ellipsoids at 50% occupancy.

desired rhenium complexes in the form of *fac*-[Re(CO)$_3$($\mathbf{L}''$)](BF$_4$) as yellow air-stable powders. Again the complexes were characterized using a range of appropriate techniques. IR spectroscopy confirmed the facial geometry (pseudo C_s) of the complexes via three CO stretching frequencies at 2030−1890 cm^{-1}, as well as the carbonyls of the coordinated ligand. HRMS produced the correct isotopic pattern expected for $^{185/187}$Re. In the ^{1}H NMR spectra both the methylene and ethylene linkers of the dipicolyl amine receptor unit shift from the corresponding free ligand. Among the aliphatic proton signals, two sets of characteristic resonances were assigned to the diastereotopic protons of the dipicolyl amine methylene linkers, possessing a coupling constant of ca. 16−18 Hz consistent with a $^2J_{HH}$ geminal coupling.[31] Remarkably, the separation between the two diastereotopic resonances was strongly dependent upon the naphthalimide structure, with $\mathbf{L}^3$ inducing the largest separation. The observation of diastereotopic protons provides categorical evidence for the proposed binding mode, rendering coordinative participation of the naphthalimide nitrogen donor unlikely.

The solution absorption spectra of $\mathbf{L}^{1-4}$ (data recorded in Table 1) were composed of at least two dominant absorptions: the pyridyl units absorb at <290 nm, while the naphthalimide chromophore absorbs at 330−450 nm. The lowest energy absorption appeared as a broad, unstructured band at ca. 437 nm ($\varepsilon \approx 10^4$ M^{-1} cm^{-1}). Comparison with the unsubstituted precursors ($\mathbf{Cl}^{1-4}$) indicated that the addition of the amine substituent clearly induced a significant bathochromic shift of the lowest energy absorption band, which was also found to be sensitive to solvent polarity. The solubility of $\mathbf{L}^3$ enabled additional measurements to be conducted on aqueous solutions, with the visible band further shifted to 449 nm. These observations are consistent with a significant intraligand charge transfer (ICT) (N-to-π^*) contribution to the transition arising from the donating amino substituent and the accepting naphthalimide unit.

Solutions of $\mathbf{L}^{1-4}$ were also found to be fluorescent (Table 1). Using an excitation wavelength of 345−425 nm on aerated MeCN and MeOH solutions of the ligands revealed a visible emission band at ca. 520 nm, which was largely insensitive to the nature of imide functionalization (Scheme 1). Again, the emission of $\mathbf{L}^3$ was also obtained in water, fluorescing at 537 nm. The moderate Stokes shift and sensitivity of λ_{em} to solvent

dx.doi.org/10.1021/ic500142z | Inorg. Chem. 2014, 53, 3788−3797

Table 1. Absorption and Fluorescence Properties of the Ligands and Complexes

structure	λ_{max}/nm[a] (ε/M^{-1}cm^{-1})	λ_{max}/nm[b] (ε/M^{-1}cm^{-1})	λ_{em}/nm[c]	λ_{em}/nm[d]	τ[e]	τ[f]	Φ[g]
L^1	439 (13 500)	445 (13 800)	523	534	2.6, 7.6 (97%)	2.8, 8.7 (83%)	
L^2	437 (13 100)	431 (12 900)	529	537	2.6, 6.4 (89%)	1.7, 5.4 (92%)	
L^3	437 (14 400)	442 (13 900)	523	530	3.7, 8.2 (90%)	2.9, 7.1 (80%)	
L^4	436 (14 900)	445 (14 200)	524	533	4.5, 8.5 (93%)	1.8, 5.1 (90%)	
Re-L^1	421 (12 800)	427 (13 100)	505	518	3.1, 9.8 (98%)	3.8, 8.8 (98%)	0.83
Re-L^2	421 (13 800)	427 (13 000)	510	514	3.2, 9.7 (96%)	3.3, 8.8 (95%)	0.57
Re-L^3	421 (12 800)	427 (15 200)	505	516	4.1, 9.8 (95%)	2.2, 8.4 (97%)	0.58
Re-L^4	420 (15 200)	427 (17 900)	506	520	9.1	8.1	0.89

[a] 10^{-5} M MeCN. [b] 10^{-5} M MeOH. [c] MeCN, λ_{ex} = 425 nm. [d] MeOH, λ_{ex} = 425 nm. [e] MeCN, λ_{ex} = 372 nm. [f] MeOH, λ_{ex} = 372 nm. [g] Aerated MeCN.

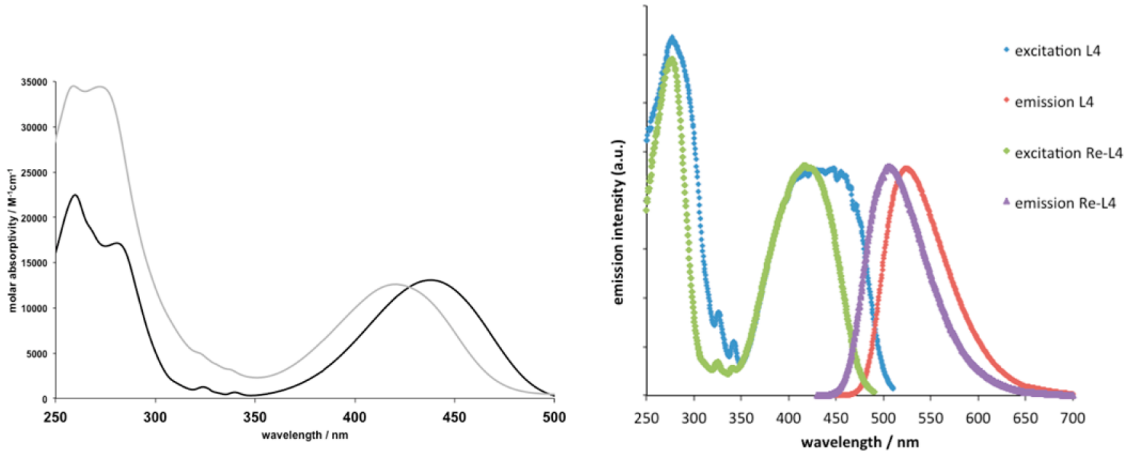

Figure 2. (left) UV–vis absorption for L^2 (black) and Re-L^2 (gray) (recorded in MeCN). (right) Normalized excitation and emission spectra for L^4 and Re-L^4 (recorded in MeCN).

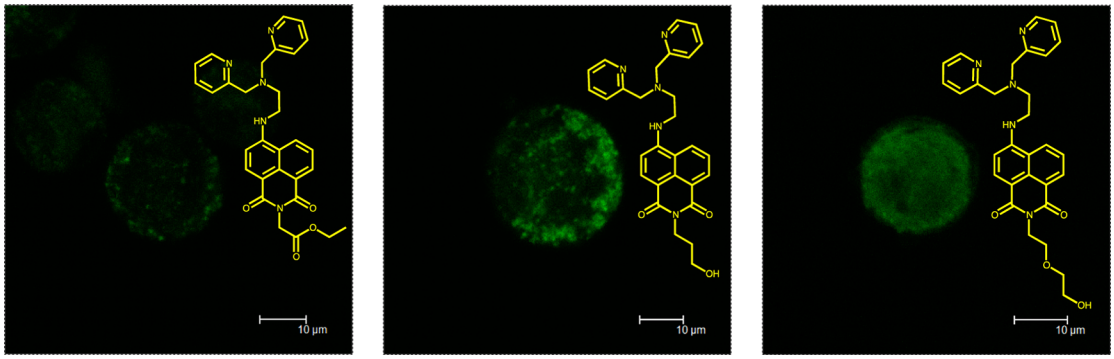

Figure 3. Confocal fluorescence microscopy of osteoarthritic cells imaged using (left to right) L^1 (poor uptake, indicative of limiting permeability), L^2 (excellent uptake, with mitochondrial localization), and L^3 (good uptake, diffusely distributed with cytoplasmic binding). All images obtained using λ_{ex} = 405 nm and λ_{em} = 535 nm.

polarity again suggests an excited state of ICT character. Time-resolved measurements showed that in the majority of cases the decay profiles fitted best to a biexponential yielding two lifetime components all of which were indicative of fluorescence (<10 ns). The dual-component decay suggests the presence of a minor, quenched species, since in all cases the longer component dominates (>80%).

Crucially, upon coordination to Re(I) each of the ligands retained these characteristic absorption and emission properties (see example spectra in Figure 2). For the complexes the absorption maximum was slightly blue-shifted to around 427 nm and thus was highly compatible with confocal fluorescence microscopy. Relative to the free ligands, hypsochromic shifts were noted for the corresponding emission wavelengths, and fluorescence lifetimes were generally extended for the complexes (Table 1). This shift may be a consequence of the overall cationic charge of the complex modulating the stability of the emitting ICT excited state.[32,33] The quantum yields for the complexes were uniformly excellent (>50%) in aerated solution, suggesting that potential quenching pathways are suppressed. The occupancy of the dipicolylamine receptor probably inhibits photoinduced electron transfer, which can account for significant quenching in amino-substituted naphthalimide chromophores, as well as enhancing the rigidity of the complex and limiting vibrational deactivating pathways.

Confocal Fluorescence Microscopy. Confocal fluorescence microscopy, used to study the fluorescence imaging capability of the free ligands (L^{1-4}) and corresponding

dx.doi.org/10.1021/ic500142z | Inorg. Chem. 2014, 53, 3788–3797

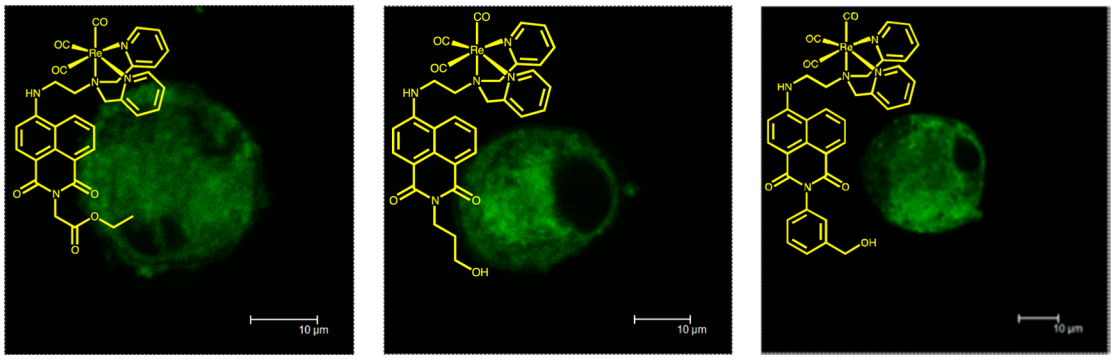

Figure 4. Confocal fluorescence microscopy of osteoarthritic cells imaged using (left to right) Re-$\mathbf{L}^1$, Re-$\mathbf{L}^2$, and Re-$\mathbf{L}^4$ (λ_{ex} = 405 nm; λ_{em} = 515 nm).

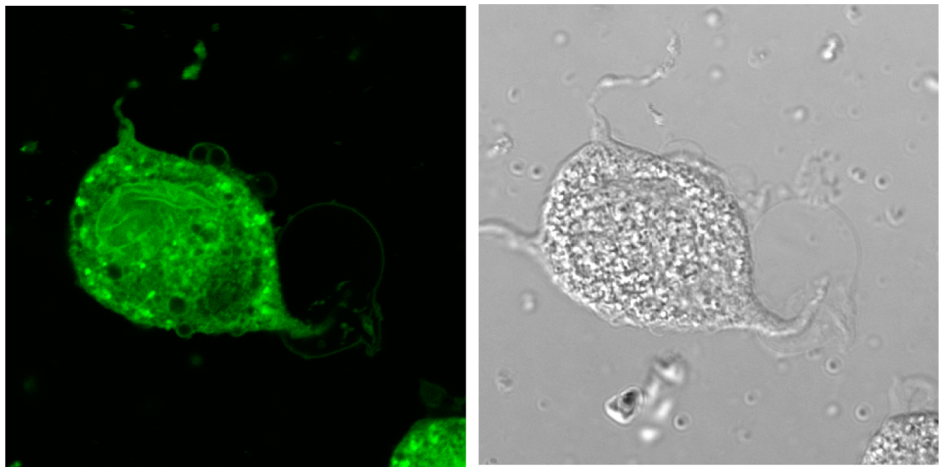

Figure 5. Microscopy images of human osteoarthritic cell undergoing apoptosis. (left) Imaged using fluorescence from Re-$\mathbf{L}^2$ (λ_{ex} = 405 nm; λ_{em} = 515 nm). (right) Imaged using trasmitted light.

complexes (Re-$\mathbf{L}^{1-4}$), was initially performed using human osteoarthritic cells. In all cases an excitation wavelength of 405 or 488 nm was used together with a detection wavelength between 515 and 535 nm (see Supporting Information, Figures S2 and S3 for autofluorescence assessments).

Comparison of the free ligands showed some remarkable differences in behavior (Figure 3). First, $\mathbf{L}^4$, which incorporates the benzyl alcohol group, did not show any uptake into the cells. $\mathbf{L}^1$ showed a reasonable uptake and a distinct granular staining pattern, possibly indicative of mitochondrial localization; no uptake in the nucleus was observed. The functionalized ligands $\mathbf{L}^2$ and $\mathbf{L}^3$ both revealed good uptake; however, no specific foci of fluorescence were noted for $\mathbf{L}^3$. This behavior contrasts with cell imaging work conducted with HepG2 (liver cancer) and HeLa cells,[16b] where $\mathbf{L}^3$ has been shown to penetrate the nuclear envelope, which may be characteristic of cells that are dying or dead.[34] The present studies clearly show that this behavior is not replicated with the osteoarthritic cell line. In comparison, $\mathbf{L}^2$ showed very distinct localization patterns with high-intensity fluorescence from mitochondrial regions. It is noteworthy that recent studies on Cu(I)-targeted detection using 4,5-disubstituted 1,8-naphthalimide probes demonstrated trans-Golgi and mitochondrial localization.[17]

Once incorporated into the architecture of the cationic rhenium complex, the variation in structures again showed vastly different imaging capability across the series (Figure 4). Despite the imaging utility of the corresponding free ligand, $\mathbf{L}^3$ surprisingly revealed the poorest uptake into the cells and was not an effective imaging fluorophore. However, the benzyl alcohol-appended Re-$\mathbf{L}^4$ showed very good uptake into the cells and bright emission, in stark contrast to $\mathbf{L}^4$, but the images show that Re-$\mathbf{L}^4$ does not cross the nuclear membrane. Re-$\mathbf{L}^1$ also showed better uptake than the corresponding free ligand, with bright emission and clear evidence of cytoplasmic membrane staining together with the selective staining of other organelles (possibly mitochondria and vacuoles). As with $\mathbf{L}^2$, the propanol-derived complex Re-$\mathbf{L}^2$ showed the most impressive uptake, yielding very bright, high-quality images. Although the complex did not detectably cross the nuclear membrane, it revealed labeling of smooth endoplasmic membranes, including those of the Golgi apparatus.

The successful identification and application of Re-$\mathbf{L}^2$ as a promising cell imaging agent led to additional studies investigating higher concentrations (4 times greater) of agent, yielding remarkably detailed images of osteoarthritic cells (Figure 5). The images provide clear evidence for rapid binding to mitochondrial membranes and other ultrastructural elements in cells undergoing apoptosis, as indicated by the extensive plasma membrane blebbing (zeiosis), cytoplasmic vacuolation, loss of cellular integrity, and, in some cases, nuclear fragmentation.

Given the quality of its imaging capability, Re-$\mathbf{L}^2$ was also selected for imaging the anaerobically grown aerotolerant protistan fish parasite *Spironucleus vortens,* where it again showed good uptake (Figure 6) and localization in the

dx.doi.org/10.1021/ic500142z | *Inorg. Chem.* 2014, 53, 3788−3797

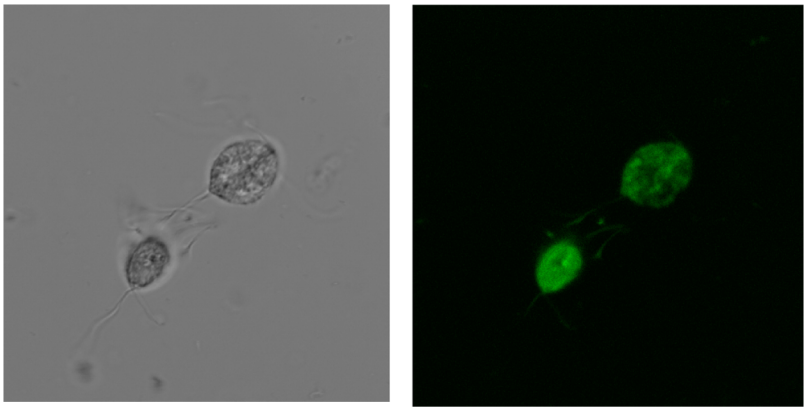

Figure 6. Microscope images of *S. vortens* incubated with Re-$\mathbf{L}^2$. (left) Normal transmission. (right) Confocal fluorescence (λ_{ex} = 405 nm; λ_{em} = 515 nm).

hydrogenosomes (redox-active organelles equivalent to the mitochondria of aerobic eukaryotic organisms). Re-$\mathbf{L}^2$ was not evidently toxic to these organisms over the duration of the entire experiment (4 h), as its rapid flagellar-driven motility and forward propulsive swimming was maintained across the entire population. Consequently, to obtain sharply focused images, it was necessary to anaesthetize using 280 mM 2,2,2-trichloroethane-1,1-diol (chloral hydrate) immediately before microscopical examination. In addition, colocalization experiments using Re-$\mathbf{L}^2$ and tetramethylrhodamine ethyl ester (TMRE) clearly showed (Figure 7) that both agents colocalize in the hydrogenosomes (secondarily derived mitochondria) of the flagellated *S. vortens*.

These imaging results present clear evidence of the biocompatible utility of these amine-substituted naphthalimide fluorophores. Importantly, it appears that the specific nature of the imide moiety can be used to tune the imaging capability of the probes, from poor uptake ($\mathbf{L}^4$) to good uptake/poor localization ($\mathbf{L}^3$), to excellent uptake and distinct granular hot spots of fluorescence ($\mathbf{L}^2$). With the exception of Re-$\mathbf{L}^3$, the cationic nature of the complexes appears to enhance cell uptake in all cases. Taken together the imaging results clearly show that simple tuning of the amphiphilic nature of the N-alkyl imide group can fundamentally alter both the uptake and localization patterns of the probes: the 3-propanol moiety appears to offer the best balance, facilitating excellent imaging capability, especially in the guise of the cationic complex Re-$\mathbf{L}^2$.

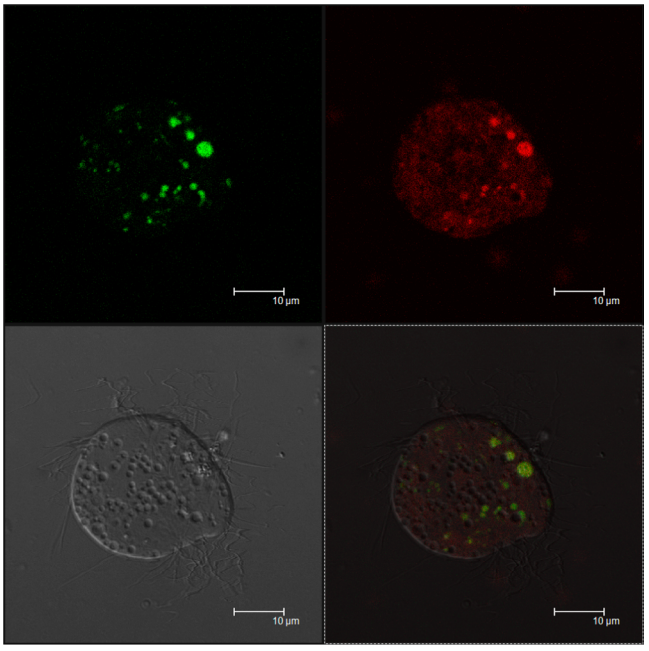

Figure 7. Microscope images of *S. vortens* incubated with Re-$\mathbf{L}^2$ and TMRE showing (clockwise from top left): green fluorescence from Re-$\mathbf{L}^2$ (λ_{ex} = 488 nm; λ_{em} = 515 nm); red fluorescence from TMRE (λ_{ex} = 543 nm; λ_{em} = 600 nm); overlaid images showing colocalization; transmission image.

In conclusion, this Paper has described the multistep synthetic development of the 1,8-naphthalimide fluorophore, generating four ligands allowing the formation of biocompatible cationic tricarbonyl rhenium complexes, where the metal ion is added at the final step. The structures vary by the amphiphilic nature of the N-alkylation of the imide compartment of the ligand structure. The optical properties are dictated by ligand-centered, intramolecular charge transfer dominated transitions that facilitate visible absorption and efficient emission characteristics, which are highly compatible with confocal fluorescence microscopy. Cellular imaging studies were conducted on both human osteoarthritic cells and *S. vortens* and showed the excellent imaging capabilities of both the ligands and complexes. Critically, the specific cellular uptake and localization characteristics can be controlled by the structure of the ligand. For the series of compounds studied here, the 3-propanol moiety of $\mathbf{L}^2$ offers the most favorable attributes regarding uptake and mitochondrial localization. Extensive cellular imaging studies with emissive lanthanide complexes have also shown that the nature of a fluorophore substituent can influence their intracellular uptake, distributions, and cytotoxicity, perhaps through varied affinities for proteins.[35] Our future studies will investigate the biological impact of further structural variations on the naphthalimide fluorophore.

To summarize, these naphthalimide-derived ligands provide a chelating site that is ideally suited to radioimaging nuclides such as ^{99m}Tc(I), while simultaneously offering the desirable physical characteristics that are biocompatible with optical cellular imaging techniques such as confocal fluorescence microscopy.

■ ASSOCIATED CONTENT

Ⓢ Supporting Information

Parameters associated with the single-crystal diffraction data collection, selected bond lengths and angles, and additional

dx.doi.org/10.1021/ic500142z | Inorg. Chem. 2014, 53, 3788−3797

confocal fluorescence microscopy imaging data. This material is free of charge via the Internet at http://pubs.acs.org. Supplementary crystallographic data are also available. These data can be obtained free of charge from the Cambridge Crystallographic Data Centre via www.ccdc.cam.ac.uk/data_request/cif.

AUTHOR INFORMATION

Corresponding Author

*E-mail: popesj@cardiff.ac.uk.

Funding

We thank Cardiff University for financial support and the staff of the EPSRC Mass Spectrometry National Service (University of Swansea) for providing MS data. We thank the EPSRC for the use of the National Crystallographic Service at the University of Southampton.

Notes

The authors declare no competing financial interest.

ACKNOWLEDGMENTS

REFERENCES

(1) (a) Dilworth, J. R.; Donnelly, P. S. Therapeutic Rhenium Radiopharmaceuticals. In *Metallotherapeutic Drugs and Metal-Based Diagnostic Agents: The Use of Metals in Medicine;* Gielen, M., Tiekink, E. R. T., Eds.; Wiley: Hoboken, NJ, 2005; p 463. (b) Cowley, A. R.; Dilworth, J. R.; Donnelly, P. S.; Ross, S. J. *Dalton Trans.* **2007**, 73−82. (c) Lambert, B.; Bacher, K.; Defreyne, L. *J. Nucl. Med. Mol. Imaging* **2009**, *53*, 305−310. (d) Dilworth, J. R.; Parrott, S. J. *Chem. Soc. Rev.* **1998**, *27*, 43−55. (e) Blower, P. J.; Dilworth, J. R.; Maurer, R. I.; Mullen, G. D.; Reynolds, C. A.; Zheng. *J. Inorg. Biochem.* **2001**, *85*, 15−22.

(2) Alberto, R.; Ortner, K.; Wheatley, N.; Schibli, R.; Schubiger, P. A. *J. Am. Chem. Soc.* **2001**, *123*, 3135−3136.

(3) (a) Stephenson, K. A.; Banerjee, S. R.; Besanger, T.; Sogbein, O. O.; Levadala, M. K.; McFarlane, N.; Lemon, J. A.; Boreham, D. R.; Maresca, K. P.; Brennan, J. D.; Babich, J. W.; Zubieta, J.; Valliant, J. F. *J. Am. Chem. Soc.* **2004**, *126*, 8598−8599. (b) Armstrong, A. F.; Lebert, J. M.; Brennan, J. D.; Valliant, J. F. *Organometallics* **2009**, *28*, 2986−2992. (c) Emerson, D. K.; Limmer, K. K.; Hall, D. J.; Han, S.-H.; Eckelman, W. C.; Kane, C. J.; Wallace, A. M.; Vera, D. R. *Radiology* **2012**, *265*, 186−193. (d) Yang, Y.; Zhu, L.; Cui, M.; Tang, R.; Zhang, H. *Bioorg. Med. Chem. Lett.* **2010**, *20*, 5337−5344.

(4) Thorp-Greenwood, F. L.; Coogan, M. P. *Dalton Trans.* **2011**, *40*, 6129−6143.

(5) For example, (a) Amoroso, A. J.; Coogan, M. P.; Dunne, J. E.; Fernandez-Moreira, V.; Hess, J. B.; Hayes, A. J.; Lloyd, D.; Millet, C.; Pope, S. J. A.; Williams, C. *Chem. Commun.* **2007**, 3066−3068. (b) Balasingham, R. G.; Thorp-Greenwood, F. L.; Williams, C. F.; Coogan, M. P.; Pope, S. J. A. *Inorg. Chem.* **2012**, *51*, 1419−1426.

(6) (a) Li, C.; Yu, M.; Sun, Y.; Wu, Y.; Huang, C.; Li, F. *J. Am. Chem. Soc.* **2011**, *133*, 11231−11239. (b) Fernandez-Moreira, V.; Thorp-Greenwood, F. L.; Coogan, M. P. *Chem. Commun.* **2010**, *46*, 186−202. (c) Lo, K.K-W.; Choi, A.W-T.; Law, W.H-T. *Dalton Trans.* **2012**, *41*, 6021−6047.

(7) Botchway, S. W.; Charnley, M.; Haycock, J. W.; Parker, A. W.; Rochester, D. L.; Weinstein, J. A.; Williams, J. A. G. *Proc. Natl. Acad. Sci. U.S.A.* **2008**, *105*, 16071−16076.

(8) (a) Hafliger, P.; Agorastos, N.; Spingler, B.; Georgiev, O.; Viola, G.; Alberto, R. *ChemBioChem* **2005**, *6*, 414−421. (b) Polyakov, V.; Sharma, V.; Dahlheimer, J. L.; Pica, C. M.; Luker, G. D.; Piwnica-Worms, D. *Bioconjugate Chem.* **2000**, *11*, 762−771. (c) Maresca, K. P.; Hillier, S. M.; Femia, F. J.; Zimmerman, C. N.; Levadala, M. K.; Banerjee, S. R.; Hicks, J.; Sundararajan, C.; Valliant, J.; Zubieta, J.; Eckelman, W. C.; Joyal, J. L.; Babich, J. W. *Bioconjugate Chem.* **2009**, *20*, 1625−1633. (d) Sagnou, M.; Tzanopoulou, S.; Raptopoulou, C. P.; Psycharis, V.; Braband, H.; Alberto, R.; Pirmettis, I. C.; Papadopoulous, M.; Pelecanou, M. *Eur. J. Inorg. Chem.* **2012**, 4279−4286.

(9) (a) Bryce, N. S.; Zhang, J. Z.; Whan, R. M.; Yamamoto, N.; Hambley, T. W. *Chem. Commun.* **2009**, 2673−2675. (b) Zhang, J. Z.; Bryce, N. S.; Lanzirotti, A.; Chen, C. K. J.; Paterson, D.; de Jonge, M. D.; Howard, D. L.; Hambley, T. W. *Metallomics* **2012**, *4*, 1209−1217.

(10) Balasingham, R. G.; Williams, C. F.; Mottram, H. J.; Coogan, M. P.; Pope, S. J. A. *Organometallics* **2012**, *31*, 5835−5843.

(11) Lakowicz, J. R. *Principles of Fluorescence Spectroscopy,* 3rd ed.; Springer: New York, 2006.

(12) (a) Gunnlaugsson, T.; Glynn, M.; Tocci, G. M.; Kruger, P. E.; Pfeffer, F. M. *Coord. Chem. Rev.* **2006**, *250*, 3094−3117. (b) Banerjee, S.; Kitchen, J. A.; Gunnlaugsson, T.; Kelly, J. M. *Org. Biomol. Chem.* **2013**, *11*, 5642−5655.

(13) (a) Li, Y.; Wu, Y.; Chang, J.; Chen, M.; Liu, R.; Li, F. *Chem. Commun.* **2013**, *49*, 11335−11337. (b) Lin, H.-H.; Chan, Y.-C.; Chen, J.-W.; Chang, C.-C. *J. Mater. Chem.* **2011**, *21*, 3170−3177. (c) Chen, L.; Li, J.; Liu, Z.; Ma, Z.; Zhang, W.; Du, L.; Xu, W.; Fang, H.; Li, M. *RSC Adv.* **2013**, *3*, 13412−13416. (d) Xie, J.; Chen, Y.; Yang, W.; Xu, D.; Zhang, K. *J. Photochem. Photobiol., A* **2011**, *223*, 111−118. (e) Ott, I.; Xu, Y.; Liu, J.; Kokoschka, M.; Harlos, M.; Sheldrick, W. S.; Qian, X. *Bioorg. Med. Chem. Lett.* **2008**, *16*, 7107−7116.

(14) Banerjee, S.; Veale, E. B.; Phelan, C. M.; Murphy, S. A.; Tocci, G. M.; Gillespie, L. J.; Frimannsson, D. O.; Kelly, J. M.; Gunnlaugsson, T. *Chem. Soc. Rev.* **2013**, *42*, 1601−1618.

(15) Selected examples: (a) Srikun, D.; Miller, E. W.; Domaille, D. W.; Chang, C. J. *J. Am. Chem. Soc.* **2008**, *130*, 4596−4597. (b) Zhu, B.; Zhang, X.; Li, Y.; Wang, P.; Zhang, H.; Zhuang, X. *Chem. Commun.* **2010**, *46*, 5710−5712. (c) Zhang, J.-F.; Kim, S.; Han, J.-H.; Lee, S.-J.; Pradhan, T.; Cao, Q. Y.; Lee, S. J.; Kang, C.; Kim, J.-S. *Org. Lett.* **2011**, *13*, 5294−5297. (d) Xu, L.; Xu, Y.; Zhu, W.; Yang, W.; Han, L.; Qian, X. *Dalton Trans.* **2012**, *41*, 7212−7217. (e) Wang, Q.; Li, C.; Zou, Y.; Wang, H.; Yi, T.; Huang, C. *Org. Biomol. Chem.* **2012**, *10*, 6740−6746. (f) Lee, M. H.; Han, J. H.; Kwon, P.-S.; Bhuniya, S.; Kim, J. Y.; Sessler, J. L.; Kang, C.; Kim, J.-S. *J. Am. Chem. Soc.* **2012**, *134*, 1316−1322. (g) Hu, X.; Zhang, X.; Song, H.; He, C.; Bao, Y.; Tang, Q.; Duan, C. *Tetrahedron* **2012**, *68*, 8371−8375.

(16) (a) Zhao, L. Y.; Mi, Q. L.; Wang, G. K.; Chen, J. H.; Zhang, J. F.; Zhao, Q. H.; Zhou, Y. *Tetrahedron Lett.* **2013**, *54*, 3353−3358. (b) During the course of our studies the synthesis of L^3 was reported via an alternative method in Zhang, C.; Liu, Z.; Li, Y.; He, W.; Gao, X.; Guo, Z. *Chem. Commun.* **2013**, *49*, 11430−11432.

(17) Satriano, C.; Sfrazzetto, G. T.; Amato, M. E.; Ballistreri, F. P.; Copani, A.; Giuffrida, M. L.; Grasso, G.; Pappalardo, A.; Rizzarelli, E.; Tomaselli, G.; Toscano, R. M. *Chem. Commun.* **2013**, *49*, 5565−5567.

(18) (a) Perez, J. M.; Lopez-Solera, I.; Montero, E. I.; Brana, M. F.; Alonso, C.; Robinson, S. P.; Navarro-Ranninger, C. *J. Med. Chem.* **1999**, *42*, 5482−5486. (b) Banerjee, S.; Kitchen, J. A.; Bright, S. A.; O'Brien, J. E.; Williams, D. C.; Kelly, J. M.; Gunnlaugsson, T. *Chem. Commun.* **2013**, *49*, 8522−8524.

(19) Bagowski, C. P.; You, Y.; Scheffler, H.; Vlecken, D. H.; Schmitz, D. J.; Ott, I. *Dalton Trans.* **2009**, 10799−10805.

(20) (a) Roy, S.; Saha, S.; Majumdar, R.; Dighe, R. R.; Chakravarty, A. R. *Inorg. Chem.* **2009**, *48*, 9501−9509. (b) Ryan, G. J.; Quinn, S.; Gunnlaugsson, T. *Inorg. Chem.* **2008**, *47*, 401−403. (c) Ryan, G. J.; Elmes, R. B. P.; Quinn, S.; Gunnlaugsson, T. *Supramol. Chem.* **2012**, *24*, 175−188. (d) Elmes, R. B. P.; Erby, M.; Bright, S. A.; Williams, D. C.; Gunnlaugsson, T. *Chem. Commun.* **2012**, *48*, 2588−2590.

(21) Kilpin, K. J.; Clavel, C. M.; Edafe, F.; Dyson, P. J. *Organometallics* **2012**, *31*, 7031−7039.

(22) Coles, S. J.; Gale, P. A. *Chem. Sci.* **2012**, *3*, 683−689.

(23) Sheldrick, G. M. *Acta Crystallogr.* **2008**, *A64*, 112−122.

(24) Farrugia, L. J. *J. Appl. Crystallogr.* **1997**, *30*, 565.

(25) (a) Frank, M.; Nieger, M.; Vogtle, F.; Belser, P.; von Zelewsky, A.; Cola, L. D.; Balzani, V.; Barigelletti, F.; Flamigni, L. *Inorg. Chim. Acta* **1996**, *242*, 281−291. (b) Juris, A.; Balzani, V.; Barigelletti, F.; Campagna, S.; Belser, P.; von Zelewsky, A. *Coord. Chem. Rev.* **1988**, *84*, 85−277.

(26) Casper, J. V.; Meyer, T. J. *J. Phys. Chem.* **1983**, *87*, 952−957.
(27) Chhabra, S. R.; Mahajan, A.; Chan, W. C. *J. Org. Chem.* **2002**, *67*, 4017−4029.
(28) Previously reported in de Oliveira, K.; Costa, P.; Santin, J.; Mazzambani, L.; Burger, C.; Mora, C.; Nunes, R.; de Souza, M. *Bioorg. Med. Chem.* **2011**, *19*, 4295−4306.
(29) Adapted from Stolarski, R. Fluorescent Naphthalimide Dyes for Polyester Fibres. In *Fibres & Textiles in Eastern Europe;* IBWCh: Lodz, Poland, 2009; Vol. *17* pp 91−95.
(30) Mullice, L. A.; Pope, S. J. A. *Dalton Trans.* **2010**, *39*, 5908−5917.
(31) Mullice, L. A.; Laye, R. H.; Harding, L. P.; Buurma, N. J.; Pope, S. J. A. *New J. Chem.* **2008**, *32*, 2140−2149.
(32) Parkesh, R.; Lee, T. C.; Gunnlaugsson, T. *Org. Biomol. Chem.* **2007**, *5*, 310−317.
(33) Veale, E. B.; Kitchen, J. A.; Gunnlaugsson, T. *Supramol. Chem.* **2013**, *25*, 101−108.
(34) New, E. J.; Parker, D. *Org. Biomol. Chem.* **2009**, *7*, 851−855.
(35) Kielar, F.; Law, G.-L.; New, E. J.; Parker, D. *Org. Biomol. Chem.* **2008**, *6*, 2256−2258.